

A high-resolution imaging algorithm based on scattered waveform estimation for UWB pulse radar systems

Shouhei KIDERA † Takuya SAKAMOTO † Toru SATO †
Tomohiko MITANI ‡ and Satoshi SUGINO ††
Dept. of Communications and Computer Eng., Kyoto University, Kyoto, 606-8501 JAPAN †
Facsimile: +81-75-753-3342 E-mail: kidera@aso.cce.i.kyoto-u.ac.jp
Research Institute for Sustainable Humansphere, Kyoto Univ., Kyoto, Japan ‡
Advanced MEMS Development Center, Matsushita Electric Works, Ltd. ††

Abstract

Target estimation methods with UWB pulse signals are promising as imaging techniques for interior robots. We have already proposed an efficient algorithm of shape estimation named SEABED (Shape Estimation Algorithm based on BST and Extraction of Directly scattered waves), which is based on a reversible transform BST (Boundary Scattering Transform) between time delay and target shapes. In this method, we take a quasi-wavefront from received signals with the matched filter of transmitted waveform in order to estimate a target shape. However, the scattered waveform is different from the transmitted waveform in general depending on the target shape. This difference causes estimation errors in SEABED method. In this report, we propose a high-resolution algorithm of polygonal-target shape estimation based on the scattered waveform estimation, and evaluate the method by numerical simulations.

keyword

UWB pulse radar, scattered wave estimation, edge diffraction, specular reflection, shape estimation, Fresnel filter

1 Introduction

Development of robot techniques is aiming at advanced robots that can measure surrounding environment. Many imaging methods using optical approach have been proposed. However, passive optical techniques suffer from an insufficient range resolution. On the other hand, radar imaging methods have a high range resolution, and they can estimate object shapes even in the case of a fire where optical methods cannot be used. In addition, radar systems can be applied to human movement detection systems where optical methods are not suitable from the viewpoint of privacy. While many imaging algorithms for radar systems have been proposed [1, 2, 3], they require intensive computation because they are based on parametric methods. To solve this problem, we proposed SEABED [4, 5], and accomplished a fast target imaging. However, this method has estimation errors because it assumes that the scattered waveform is the same as the transmitted one. In this report, we propose estimation methods of scattered waveforms for a polygonal target to solve this problem. We evaluate

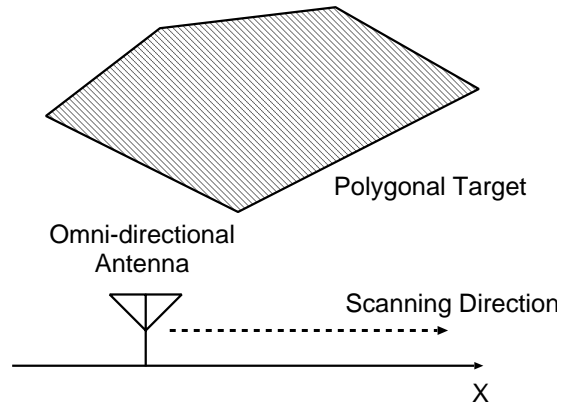


Figure 1: System Model.

the proposed methods by numerical simulations and experiments.

2 System Model

We show the system model in Fig. 1. We assume a mono-static radar system. An omni-directional antenna is scanned along a straight line. We deal with 2-dimensional problems and TE mode waves. The current is a mono-cycle pulse in the transmitting antenna. The target shape is a polygonal pillar. We assume a non-dispersive and lossless medium and the target is a perfect conductor. The spatial scale is normalized by the center wavelength of the transmitted current waveform, and the time scale is normalized by its period. In this model, we scan an antenna along x axis. We apply a matched-filter to received signals for estimating the time of arrival.

3 Target shape estimation method

In this section, we first examine scattered waveforms. Next, we introduce an algorithm of shape estimation method using an scattered waveform estimation [6].

In general, the scattered waveform from a planar boundary has the same waveform as the transmitted one with the opposite sign. The scattered waveform from a ridge of a plate has an integral waveform of the transmitted one. We show example waveforms in Fig. 2. The general scattered waveform from the boundary of the polygonal pillar is generated from these two waveforms in principle. SEABED algorithm

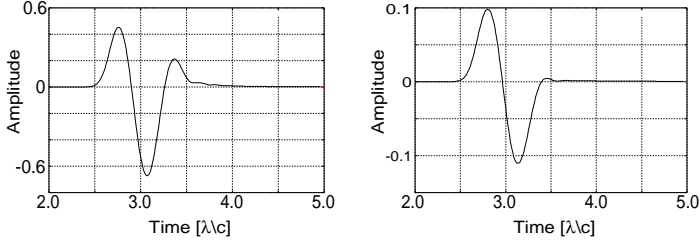


Figure 2: Left: Specular reflection waveform, Right: Edge diffraction waveform.

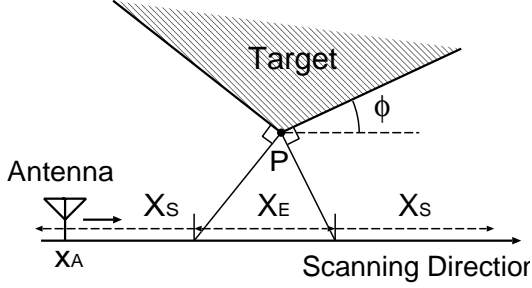


Figure 3: Arrangement of the target location and antenna.

has an estimation error caused by the waveform differences because it utilizes the matched filter for the transmitted waveform. Therefore, we should estimate scattered waveforms to enhance the accuracy.

Next, we propose a target shape estimation method with a waveform estimation. We define the shape parameter as \mathbf{p} , which expresses the edge position and ϕ which expresses the angular of the specular boundary to the scanning direction. At first, we obtain the shape parameters by the initial shape estimation without waveform estimation. We define the antenna location as \mathbf{x}_A . With the shape parameter we determine the scanning range X_S where specular reflection is dominant and X_E where edge diffraction is dominant as shown in Fig 3. We utilize the specular waveform estimation for $\mathbf{x}_A \in X_S$ and the edge diffraction waveform estimation for $\mathbf{x}_A \in X_E$. We define the estimated waveform in each antenna location as $F(\omega)$ in the frequency domain. We estimate the time of arrival by the following equation with $F(\omega)$.

$$\tau(\mathbf{x}_A)^i = \arg \max_{\tau} \left| \int_{-\infty}^{\infty} R(\omega) F^i(\omega)^* e^{j\omega\tau} d\omega \right|, \quad (1)$$

where i expresses the number of the iteration, and $R(\omega)$ is the received waveform in the frequency domain.

We set $\mathbf{x}_A = (x_A, 0)$ because the antenna scans along x axis. We calculate \mathbf{p} and ϕ for $\mathbf{x}_A \in X_E$ and $\mathbf{x}_A \in X_S$, respectively, by utilizing estimated $\tau(\mathbf{x}_A)$. We then renew the shape parameters again. We iterate these procedures and accomplish the target shape estimation. Fig. 4 shows the flowchart of this procedure.

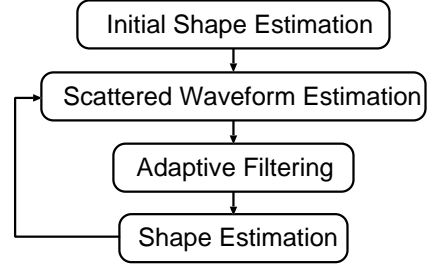


Figure 4: Flowchart of algorithm.

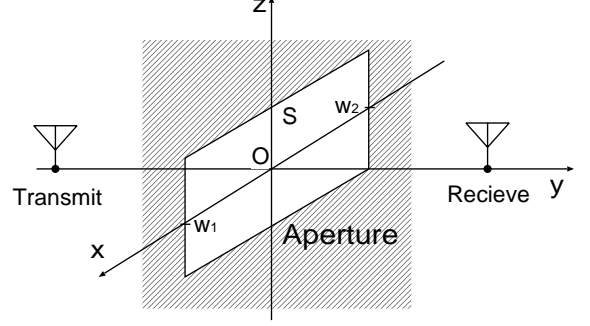


Figure 5: Arrangement of the antenna and the rectangular aperture.

4 Waveform estimation with Green's function

In this section, we express electric fields with Green's function. This idea can enhance the estimation accuracy of waveforms. At first, let us consider the electric-field waveform after propagating through a finite aperture. This model is an approximation of scattering of a rectangular target. In a 3-dimensional problem, the electric field of the wave propagating through an aperture is expressed by the following equation [7].

$$4\pi\mathbf{E}(\mathbf{r}) = (1/j\omega\epsilon) \int_C \nabla' g \mathbf{H} \cdot d\mathbf{s} + \int_C g \mathbf{E} \times d\mathbf{s} - \int_S [\mathbf{E} \partial g / \partial n - g(\partial \mathbf{E} / \partial n)] dS, \quad (2)$$

where C is the boundary of the aperture, S is the surface of the aperture, g is the Green's function, $\mathbf{E}(\mathbf{r})$ is the electric field at the position vector \mathbf{r} , and $'$ denotes the region containing sources. We take the coordinates shown in Fig. 5 and set the aperture on $y = 0$ plane. In this method, we assume that the electromagnetic field on the aperture has the uniform phase and amplitude and the distance from aperture is enough longer than a wavelength. In this assumption, we can unfold $\nabla' \simeq -\hat{y} \partial / \partial y$, $g \simeq e^{-jk y}$ and remove the first and second terms of Eq. (2). In the 3rd term we can expand $\partial g / \partial n = -\partial g / \partial y = jk g$ and $\partial \mathbf{E}(\mathbf{r}) / \partial n = -\partial \mathbf{E}(\mathbf{r}) / \partial y = -jk \mathbf{E}(\mathbf{r})$.

Finally, Eq. (2) is approximated as

$$\mathbf{E}(\mathbf{r}) = \frac{jk}{2\pi} \int_S g \mathbf{E}_0 dS, \quad (3)$$

where $E(\mathbf{r})$ is the amplitude of $\mathbf{E}(\mathbf{r})$, and E_0 is the electric field of the aperture. In a 2-dimensional prob-

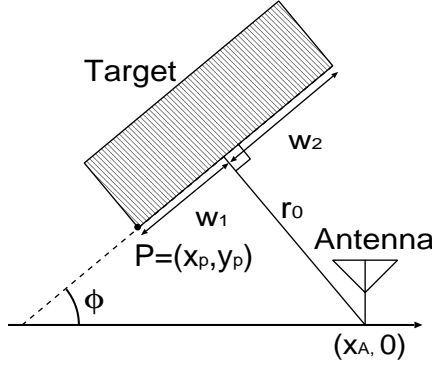


Figure 6: Arrangement of the target location and the antenna in the specular waveform region.

lem, Eq. (3) is expressed as

$$E(r) = \sqrt{\frac{jk}{2\pi}} \int_{w_1}^{w_2} g E_0 dx, \quad (4)$$

where $r = |\mathbf{r}|$, and w_1 , w_2 are the width of the aperture in a 2-dimensional problem. This equation can be used for both of specular reflection and edge diffraction waveform estimations.

5 Waveform estimation algorithms for shape estimation

5.1 Estimation of specular reflection waveforms with Green's function

The specular waveform from the planar boundary whose width is on the order of a wavelength has a frequency dependence. This is because the Fresnel zone size in the high frequency domain is relatively smaller than one in the low frequency domain. To accomplish an accurate estimation, we need to estimate the specular reflection waveform.

In this section, we propose the waveform estimation method with the Fresnel filter. We assume that the specular waveform can be approximated as the waveform after propagating through a finite aperture. We propose a specular waveform estimation based on this approximation. Here, we simplify $g(\rho) \simeq \frac{1}{\sqrt{\rho}} e^{-jk\rho}$ in Eq. (4). In this case, we can derive the following equation as

$$F_S(\omega) = E_0(\omega) e^{-jk r_0} \sqrt{\frac{j}{\pi}} \int_{\xi_1}^{\xi_2} e^{-jt^2} dt, \quad (5)$$

$$\begin{cases} \xi_1 = -\sqrt{\frac{\omega}{r_0 c}} w_1 \\ \xi_2 = \sqrt{\frac{\omega}{r_0 c}} w_2, \end{cases}$$

where we assume that $E_0(\omega)$ is the same waveform as the transmitted one with the opposite sign, and w_1 , w_2 , r_0 are estimated as

$$r_0 = \frac{|\tan \phi (x_A - x_p) + y_p|}{\sqrt{1 + \tan^2 \phi}}, \quad (6)$$

$$w_1 = \sqrt{|x_A - \mathbf{p}|^2 - r_0^2}, \quad (7)$$

$$w_2 = w - w_1, \quad (8)$$

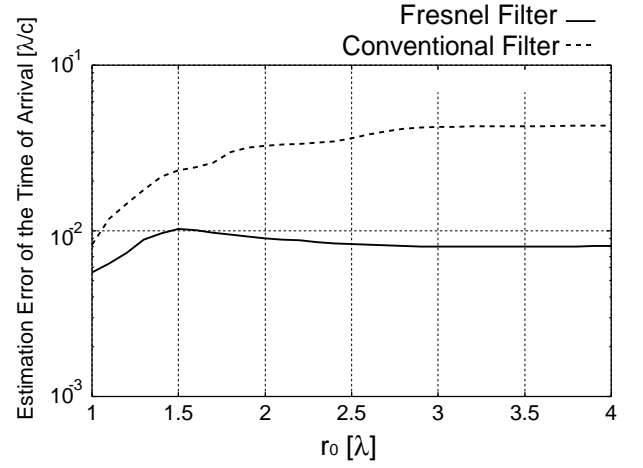


Figure 7: Estimation error of the time of arrival for $w_1 = w_2 = 0.5\lambda$.

where we define $\mathbf{p} = (x_p, y_p)$ which is the estimated edge position in the previous step. We show the target and the antenna location in Fig. 6

Fig. 7 shows the estimation error of the time of arrival versus r_0 . Here, we set $w_1 = w_2 = 0.5\lambda$. The solid line shows the error with the matched filter for $F_S(\omega)$. The broken line shows the error with the matched filter for the transmitted waveform. As shown in this figure, we confirm improvements in the arrival time accuracy compared with the conventional method. This is because the Fresnel filter correctly estimates the frequency dependence of the scattered waveform.

5.2 Estimation of specular reflection waveforms for small targets

In the previous section, we proposed the specular waveform estimation method with the Fresnel filter. However, we still have a problem that we cannot obtain an enough resolution in the time of arrival if the width of the specular boundary is smaller than a wavelength. Especially, at the tip of the specular boundary we observe strongly interfered waveforms by the edge diffraction. To solve this problem, we modify the specular waveform estimation method with the Fresnel filter and HPF (High Pass Filter).

We utilize $F_S(\omega)W(\omega)$ instead of $F_S(\omega)$, where

$$W(\omega) = \begin{cases} 1 & (\omega_h \leq \omega) \\ 0 & (\text{otherwise}) \end{cases},$$

ω_h is the cut-off angular frequency of HPF. First, we estimate the initial time of arrival τ_1 with the matched filter for $F_S(\omega)$. Second, we obtain the estimated time of arrival with the matched filter for $F_S(\omega)W(\omega)$. This operation enables us to eliminate the edge diffraction waves which has relatively low frequency components.

In HPF method, the noise tolerance is inferior to the method without HPF because we suppress the central frequency which has the maximum power of the signal. To solve this problem, we introduce the Fresnel zone index a which expresses the spatial scale normalized by the propagation distance and the wavelength. We calculate the cut-off angular frequency ω_h

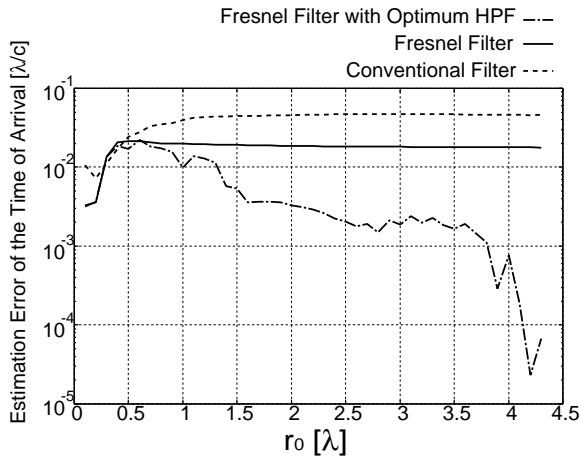


Figure 8: Estimation error of the time of arrival in Fresnel filter with optimum HPF for $w_1 = w_2 = 0.25\lambda$.

corresponding to a as

$$\omega_h = \begin{cases} 2\pi a \frac{r_0 c}{(w_1 + w_2)^2} \left(\frac{w_2}{w_1}\right)^2 & (w_2 \geq w_1) \\ 2\pi a \frac{r_0 c}{(w_1 + w_2)^2} \left(\frac{w_1}{w_2}\right)^2 & (w_2 < w_1) \end{cases}, \quad (9)$$

where r_0 , w_1 , w_2 are shown in Fig. 6. Eq. (9) enables us to determine ω_h considering the distance from the edge and preserve the signal power where the edge diffraction is not dominant.

In order to determine an optimum Fresnel zone index, we define the evaluation value as $v = \lambda(a)/P(a)$, where $\lambda(a)$ is the average of the estimated time accuracy for various sets of (w_1, w_2, r_0) , and $P(a)$ is the filtered signal power. We minimize v , and obtain the optimum value of $a = 0.27$. We make the HPF with the cut-off frequency corresponding to the optimum Fresnel zone index.

Fig. 8 shows the estimation error of the time of arrival at $w_1 = w_2 = 0.25\lambda$. The solid and broken lines are the same as Fig. 7, and the chain line expresses the estimation method by the Fresnel filter with the optimum HPF. In this figure, we obtain about 10 times improvement in the estimation accuracy for $r_0 \geq 2.5\lambda$. This is caused by the suppression of the low-frequency component by the HPF which contains the edge diffraction interference.

5.3 Estimation of Edge diffraction waveform with Green's function

We have already proposed an edge diffraction waveform estimation method with the waveform library [8]. However, this method does not consider the target width due to the limitation of the size of the libraries. Therefore, it suffers from estimation errors caused by the assumption that the size of the specular boundaries is infinite. In this section, we introduce a waveform estimation from the edge which is made by two specular boundaries of finite lengths. By expanding Eq. (4), the edge diffraction waveform is approximately expressed as

$$F(\omega) = \sqrt{\frac{jk}{2\pi}} E_0(\omega) \sum_{i=1}^2 \int_{w_{i,1}}^{w_{i,2}} g(\rho) dx, \quad (10)$$

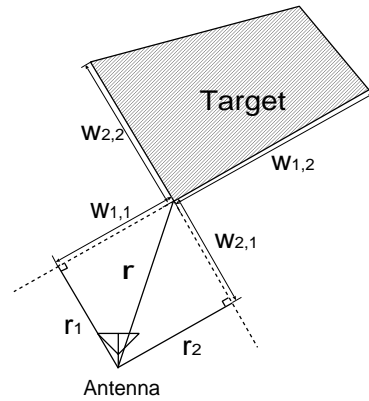


Figure 9: Arrangement of the target location and the antenna in the edge diffraction waveform region.

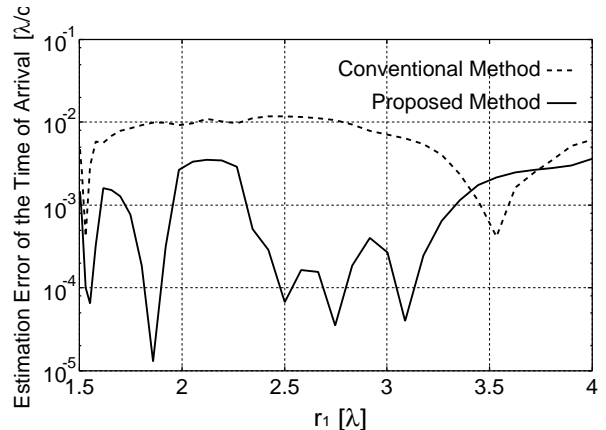


Figure 10: Estimation time error for the edge diffraction wave.

$$\rho = 2\sqrt{r_i^2 + x^2} \quad (i = 1, 2),$$

where $E_0(\omega)$ is the transmitted waveform with the opposite sign in the frequency domain, and r_i , $w_{1,i}$, $w_{2,i}$ ($i = 1, 2$) is shown in Fig. 9. $g(\rho)$ is the Green's function of 2-dimensional problem as given by

$$g(\rho) = \frac{1}{4j} H_0^{(2)}(k\rho), \quad (11)$$

where $H_0^{(2)}(x)$ is the 0th order Hankel's function of the 2nd kind, and ρ is the propagation distance. This method enables us to estimate the edge diffraction waveform considering the width of the specular boundaries making edge.

Next, we examine the estimation errors of the time of arrival in the edge waveform estimation. In Fig. 10, we show the estimation error of the time of arrival for $w_1 = w_2 = 1.0\lambda$ and $r_2 = 1.0\lambda$. The horizontal axis is r_1 . The broken line expresses the method of waveform library, and the solid line expresses the proposed method. We can confirm about 5 times improvement from the conventional method. This is because the proposed method includes the target width parameter in Eq. (10).

6 Evaluation of target shape estimation accuracy

6.1 Evaluation in Numerical simulation

We evaluate the accuracy of the proposed method by numerical simulations in this section. At first, we

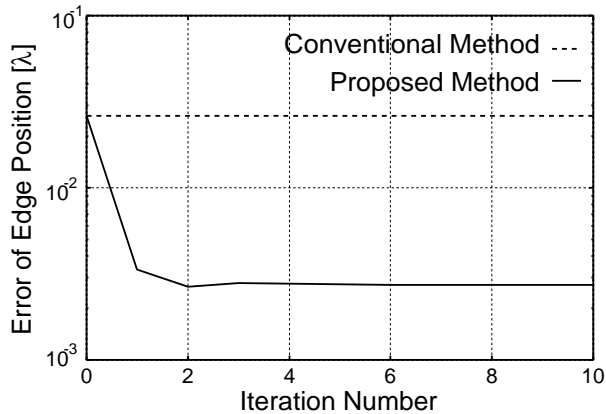


Figure 11: Estimation error of the edge location.

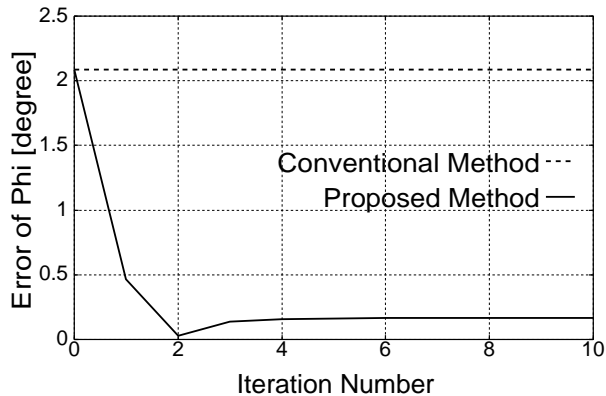


Figure 12: Estimation error of the target angle.

assume a noiseless environment. Figs. 11 and 12 show estimation error of the edge position and the target angle, respectively. The solid line and the broken line show the target shape estimation method with and without waveform estimation, respectively. As shown in these two figure, we see that we obtain a remarkable improvement in the estimation accuracy of the edge position and the target angle. Secondly, we evaluate the proposed method in a noisy environment. Fig. 13 shows the estimation error of the edge position. The lines are the same in Fig 11. In this figure, we conclude that the proposed method can largely improve the accuracy if S/N is higher than 5dB.

6.2 Evaluation in experiment

In this section, we examine the proposed method by experiments. We use the UWB signal with center frequency of 3.7 GHz and the bandwidth of 1.0 GHz. The antenna has an elliptic polarization whose ratio of the major axis to the minor one is about 10 dB.

Fig. 14 shows the location of the antenna and the target. We use a bi-static antenna whose separation in x direction is 65mm. In a 2-dimensional problem, the target length in the y direction is enough longer than the wavelength. Furthermore, we scan the transmitting antenna in the y direction as shown in Fig. 14. to obtain a 2-dimensional waveform. We calculate the 2-dimensional scattered waveform $R(x_A, t)$ as

$$R(x_A, t) = \sum_{i=0}^N r(x_A, y_i, t) \delta y, \quad (12)$$

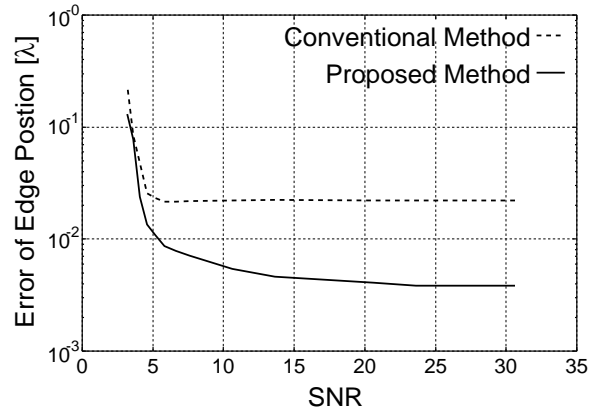


Figure 13: Estimation Error of the edge location versus SN ratio.

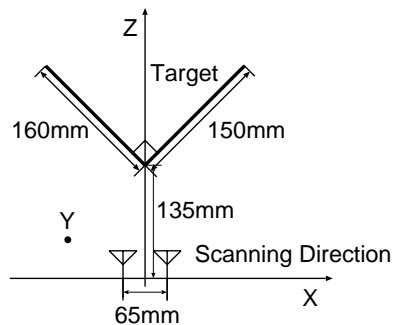


Figure 14: Arrangement of the antenna and the target in the experiment.

where $r(x_A, y_i, t)$ is the scattered waveform from the transmitting point (x_A, y_i) to the receiving point $(x_A, 0)$, N is fixed at 40, and δy is the sampling interval fixed at 10mm. We scan the transmitting antenna for the range of $-200\text{mm} \leq y \leq 200\text{mm}$.

Fig. 15 shows the estimated waveform at $x_A = 0$. The solid line expresses the scattered waveform in the experiment, the broken line expresses the transmitted waveform, and the chain line expresses the estimated waveform. As shown in this figure, the estimated waveform is much closer to the scattered waveform than the transmitted waveform. Fig. 16 shows the estimation error of the time of arrival. The solid line shows the proposed method with waveform estimation, and the broken line shows the conventional method without waveform estimation. To apply the assumption of the line polarization in the proposed method, we limit the range of scanning to $-80\text{mm} \leq x_A \leq 80\text{mm}$. In this figure, we confirm about 3 times improvement in the accuracy of time-of-arrival estimation compared to the conventional method. We also confirm that the accuracy of the edge position improves by about 3 times compared to the conventional method.

7 Conclusion

We proposed a target shape estimation method with the scattered waveform estimation. At first, we showed an iterative algorithm for target shape estimation. In the waveform estimation, we proposed the specular waveform estimation by the Fresnel filter. In addition, we applied the HPF to the Fresnel filter in

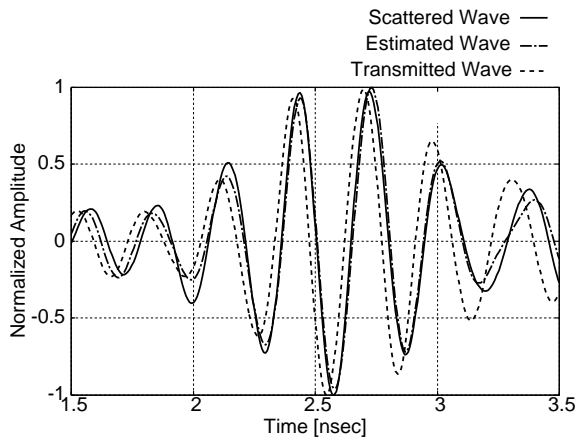


Figure 15: Scattered and estimated waveforms in the experiment.

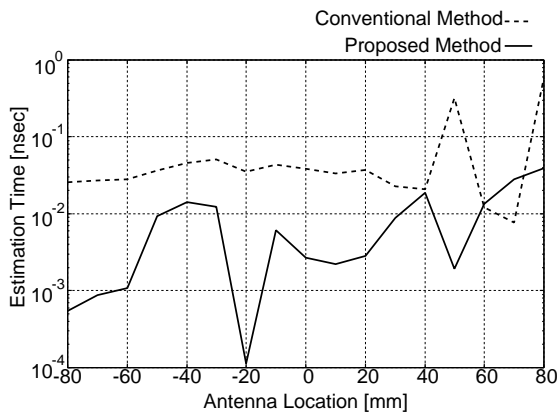


Figure 16: Estimation error of the time of arrival in experiment.

the case of a strong interference of the edge diffraction wave and we optimized the cut-off frequency in the signal power and the estimation accuracy. We proposed the edge waveform estimation. This method provides a much higher accuracy of the time-of-arrival estimation compared to a conventional waveform library method. We evaluated the accuracy in noiseless and noisy environments by numerical simulations. In the experiments we confirmed a noticeable improvement of the proposed method as far as $S/N > 15\text{dB}$. Here, we focused on a 2-dimensional problem of a polygonal pillar. We plan to expand the proposed method to an arbitrary target in a 3-dimensional problem.

References

- [1] D. Nahamoo, S. X. Pan and A. C. Kak, "Synthetic aperture diffraction tomography and its interpolation-free computer implementation," *IEEE Trans. Sonics and Ultra-sonics*, vol.31, no.4, pp.218–229, 1984.
- [2] T. Sato, K. Takeda, T. Nagamatsu, T. Wakayama, I. Kimura and T. Shinbo, "Automatic signal processing of front monitor radar for tunneling machines," *IEEE Trans. Geosci. Remote Sens.*, vol.35, no.2, pp.354–359, 1997.
- [3] T. Sato, T. Wakayama, and K. Takemura, "An imaging algorithm of objects embedded in a lossy

dispersive medium for subsurface radar data processing," *IEEE Trans. Geosci. Remote Sens.*, vol.38, no.1, pp.296–303, 2000.

- [4] T. Sakamoto and T. Sato, "A target shape estimation algorithm for pulse radar systems based on boundary scattering transform," *IEICE Trans. Commun.*, vol.E87-B, no.5, pp. 1357–1365, 2004.
- [5] T. Sakamoto and T. Sato, "A phase compensation algorithm for high-resolution pulse radar systems," *IEICE Trans. Commun.*, vol.E87-B, no.6, pp. 1631–1638, 2004.
- [6] T. Sakamoto and T. Sato, "An estimation algorithm of target location and scattered waveform for UWB pulse radar systems," *IEICE Trans. Commun.*, vol.E87-B, no.6, pp. 1631–1638, 2004.
- [7] K. Maeda and I. Kimura, *The Ohm Corp.*, 1984, pp.70–72, (in Japanese).
- [8] S. Kidera, T. Sakamoto and T. Sato, "A high-resolution algorithm of target shape estimation for UWB pulse radar systems", *IEICE, AP, Conference, National Defence Academy in Japan*, Sep, 2004, (in Japanese).

Appendix: Calculation method for the cut-off frequency by the Fresnel zone index

The Fresnel zone is the size of the aperture normalized by the propagation wavelength and the distance. This size expressed as the Fresnel-zone index a by following equation.

$$a = \frac{w^2}{\lambda r}, \quad (13)$$

where λ is the wavelength, r is the propagation distance, and w is the size of the aperture. The cut-off frequency for the Fresnel-index is expressed by the following equation.

$$\omega_h = 2\pi a \frac{rc}{w^2}. \quad (14)$$

Considering the distance from the edge of the aperture, we define the cut-off frequency as

$$\omega_h = \begin{cases} 2\pi a \frac{rc}{(w_1 + w_2)^2} \left(\frac{w_2}{w_1}\right)^2 & (w_2 \geq w_1) \\ 2\pi a \frac{rc}{(w_1 + w_2)^2} \left(\frac{w_1}{w_2}\right)^2 & (w_2 < w_1) \end{cases}, \quad (15)$$

where r , w_1 , w_2 are shown in Fig.6.